# Water-Soluble Copolymers. 18. Copolymers of Acrylamide with Sodium 3-Methacrylamido-3-methylbutanoate: Microstructural Studies and Solution Properties

**C. L. McCormick,* D. L. Elliott, and K. P. Blackmon**

*Department of Polymer Science, University of Southern Mississippi, Hattiesburg, Mississippi 39406.* *Received November 19, 1985*

ABSTRACT: Dilute solution properties of copolymers of acrylamide (AM) with sodium 3-methacrylamido-3-methylbutanoate (NaMAMB) of known molecular weight have been studied as a function of composition, temperature, time, pH, and added electrolytes. Microstructural analyses have been performed with $^{13}C$ NMR and statistical methods. Potentiometric and turbidimetric properties have been studied and correlated with the structural data. The copolymers exhibit moderate solution viscosities and viscosity–temperature coefficients in water. The AM–NaMAMB copolymers exhibit large reductions in viscosity as a function of increasing ionic strength; furthermore, no phase separation in the presence of divalent ions is observed up to 100 °C. These properties can be related to polymer microstructure, which allows favorable hydrogen bonding and charge–charge interactions to occur along the macromolecular backbone.

## Introduction

Water-soluble polymers of acrylamide (AM) are of growing importance for a variety of industrial applications, including enhanced oil recovery.[1] However, a serious limitation of many polyelectrolytes, including those derived from hydrolyzing polyacrylamide, is the large reduction in solution viscosity due to the addition of electrolytes, increased temperature, and changes in pH. In addition, phase separation in the presence of divalent ions is a major problem.[2,3]

The aim of our continuing research is to prepare model water-soluble polymers with large hydrodynamic dimensions in electrolyte solutions that are stable against phase separation in the presence of divalent ions, e.g., $CaCl_2$. In two previous papers[4,5] we reported the synthesis, characterization, and solution properties of copolymers of AM with sodium 3-acrylamido-3-methylbutanoate (NaAMB). These AM–NaAMB copolymers were found to exhibit high solution viscosities, good salt tolerance, and resistance to phase separation in electrolyte solutions.

We have previously reported that the microstructure of a copolymer will significantly affect its potentiometric properties.[5,6] In the AM–NaMAMB copolymers, we have attempted to compare directly the copolymer sequence distributions (CSD) calculated by the method of Harwood and Ritchey[7] to NMR data on experimentally prepared copolymers. We now report the viscometry, potentiometry, turbidimetry, and $^{13}C$ NMR analysis of these copolymers of AM and NaMAMB in order to relate the observed solution properties to the polymer microstructure.

## Experimental Section

**Materials.** Copolymers of acrylamide (AM) with sodium 3-methacrylamido-3-methylbutanoate (NaMAMB) were prepared at 30 °C in aqueous solution at pH 9 using potassium persulfate as the initiator. Details of the synthesis, purification, and characterization procedures have been reported in the previous paper.[18] The polymers were freeze-dried and stored in a vacuum desiccator until used.

Reagent-grade sodium chloride from J. T. Baker Co. was used without purification. Calcium chloride from J. T. Baker Co. was dissolved in water, filtered, and dried at 175 °C prior to use. All aqueous salt solutions were prepared within deionized water.

**Characterization.** The copolymer compositions of all polymers were determined from elemental analysis and $^{13}C$ NMR. Microstructures (Table I) were calculated with the statistical method[8] as described in the previous paper.[18]

**Viscosity Measurements.** Stock solutions of sodium chloride (0.043, 0.257, 0.514, and 1.0 M NaCl) were prepared by dissolving the appropriate amount of salt in deionized water in volumetric flasks. The required quantities of the dry copolymers were dissolved in the salt solutions. The dissolution process was generally complete within 1 day. Care was taken to avoid excessive shear during dissolution of the polymers.

Solution viscosities were measured in a Cannon–Ubbelohde four-bulb shear dilution capillary viscometer (size 100). The shear rate constants and viscometer constants were provided by the manufacturer. The Carreau model[9] was used to obtain zero-shear viscosities by extrapolation of apparent viscosities to zero shear rate. The Huggins equation[10] was then used to obtain zero-shear intrinsic viscosities, $[\eta]_0$, by extrapolation of the reduced viscosity, $\eta_{sp}/c$, to infinite dilution.

**Turbidimetric Measurements.** The method used to study the phase separation of these copolymers has been reported previously.[11,12] Calcium chloride solutions were prepared gravimetrically and the concentrations were verified by refractive index measurements. Polymer solutions were prepared by dissolving the appropriate amount of polymer in deionized water. Polymer solution concentrations were 1.5 g/L. Salt concentrations were varied by addition of solid salt for higher concentrations or known amounts of salt solution for lower concentrations. The weight of the solution was determined both before and after each measurement, and water lost by evaporation was replaced. The measurements were repeatable to within ±0.5 °C.

**Potentiometric Measurements.** The procedure for the potentiometric measurements has been reported previously.[5,6,13] Measurements were made with a Corning 130 pH–mV meter with an Orion pH electrode. Measurements were conducted at 25 ± 0.05 °C.

Polymer concentrations were 1.5 g/L. Each sample was titrated at constant ionic strength (0.36 M KCl) and with no ionic strength adjustment. The titrations were conducted under nitrogen atmosphere with dilute acid solutions (<0.1 M). The degree of ionization was measured as reported previously.[5,6,13] Values of $pK_a$ (dissociation constant) were calculated with the modified Henderson–Hasselbalch equation[14]

$$pH = pK' + n \log (\alpha/1 - \alpha) \quad (1)$$

The values reported are apparent $pK_a$ values. The degree of electrostatic repulsion was also studied with the $n$ value of the modified Henderson–Hasselbalch equation.

**$^{13}C$ NMR Spectroscopy.** Polymer solutions for NMR experiments were prepared by weighing the appropriate amount of dried polymer and adding it to 2 mL of $D_2O$ in a 10-mm-o.d. tube. Concentrations ranged from 5 to 8% (w/v). Dissolution was accomplished in a 3-day period.

All NMR spectra were obtained on a JEOL FX90Q spectrometer operating at a $^{13}C$ NMR frequency of 22.5 MHz. Exponential weighting was employed by using typically a 5000-Hz window. The spectra were referenced with an external DSS standard. The probe temperature was maintained at 32 ± 2 °C.

## Results and Discussion

**Aging Effects.** In order to properly assess the effects of temperature, added electrolytes, copolymer composition, and pH on the solution behavior of the AM–NaMAMB

0024-9297/86/2219-1516$01.50/0 

**Table I**
**Structural Data for the Copolymers of Acrylamide (AM) with Sodium 3-Methacrylamido-3-methylbutanoate (NaMAMB)**

| sample | composn,[a] mol % | | blockiness,[b] mol % | | AM–Na-MAMB alternation,[b] mol % | mean sequence length | |
|---|---|---|---|---|---|---|---|
| | AM | NaMAMB | AM–AM | NaMAMB–NaMAMB | | $\mu_{AM}$ | $\mu_{NaMAMB}$ |
| MAMB-10-1 | 84.2 | 15.8 | 69.2 | 0.8 | 30.0 | 5.5 | 1.1 |
| MAMB-25-1 | 68.1 | 31.9 | 40.6 | 4.4 | 55.0 | 2.5 | 1.2 |
| MAMB-40-1 | 56.6 | 43.4 | 24.0 | 10.7 | 65.3 | 1.8 | 1.3 |
| MAMB-60-1 | 44.5 | 55.5 | 11.6 | 22.5 | 65.9 | 1.3 | 1.7 |
| MAMB-75-1 | 31.8 | 68.2 | 4.4 | 40.8 | 54.8 | 1.2 | 2.4 |

[a] From elemental analysis. [b] Statistically calculated with reactivity ratios.

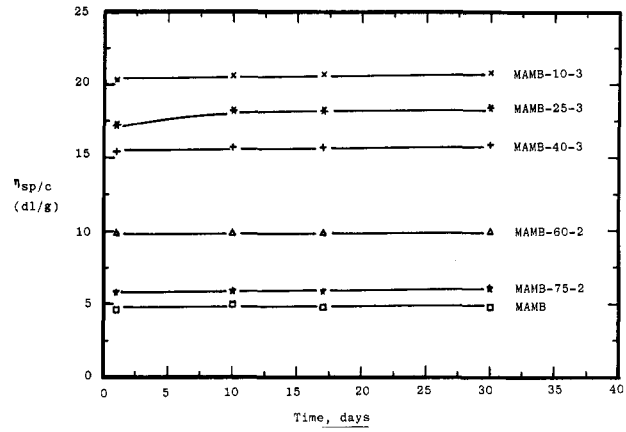


**Figure 1.** Aging of AM–NaMAMB copolymers and NaMAMB homopolymer in 0.257 M NaCl(aq) at 30 °C.

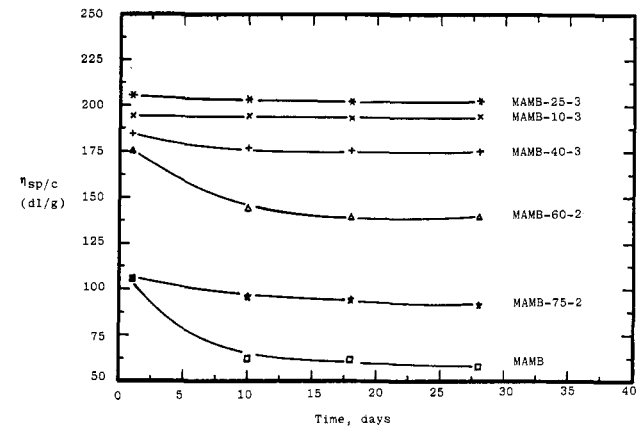


**Figure 2.** Aging of AM–NaMAMB copolymers and NaMAMB homopolymer in deionized water at 30 °C.

polymers, aging studies were first conducted. For aqueous solutions of many water-soluble polymers, including polyelectrolytes, the effects of aging are seen in an initial increase in measured viscosity during dissolution followed by a gradual viscosity decrease. Such an aging effect has been observed for polyacrylamide[15] and partially hydrolyzed polyacrylamide[16] and may be attributed to conformational changes resulting from changes in inter- and intrachain hydrogen bonding in aqueous solutions.

The aging effects for the AM–NaMAMB copolymers and NaMAMB homopolymer were studied by utilizing a size 100 Cannon–Fenske capillary viscometer at 30 °C. The polymer concentrations in 0.257 M NaCl were 0.1 g/dL, while the polymer concentrations in deionized water were 0.03 g/dL. Figure 1 shows the aging effect for the AM–NaMAMB polymers in 0.257 M NaCl solutions. The reduced viscosities of the polymers did not decrease over the 30-day aging period; in fact, slight increases in viscosities (1–7%) were observed. Figure 2 shows the aging effect on the polymers in deionized water. For several of the AM–NaMAMB copolymers, the viscosity decreases were negligible (<5%). However, the copolymers containing the largest amounts of NaMAMB, as well as the NaMAMB homopolymer, underwent significant aging effects in deionized water. A viscosity decrease of 45% was noted for the homopolymer over the 30-day aging period. The presence of salt apparently stabilizes the charges on the polymer, preventing major conformational and/or hydrogen bonding changes that would lead to a diminished hydrodynamic volume as a function of time.

**Effects of Added Electrolytes on Intrinsic Viscosity.** The effects of added sodium chloride on the zero-shear intrinsic viscosities of the AM–NaMAMB copolymers and homopolymer are shown in Figures 3 and 4. Since the copolymers of AM with NaMAMB are polyelectrolytes, the expected viscosity decrease due to shielding of ionic charges by increasing NaCl concentration was observed. MAMB-10-3, which contains 12.1 mol % NaMAMB, exhibited the greatest degree of salt tolerance with a viscosity decrease of 57% over the studied range of salt concen-

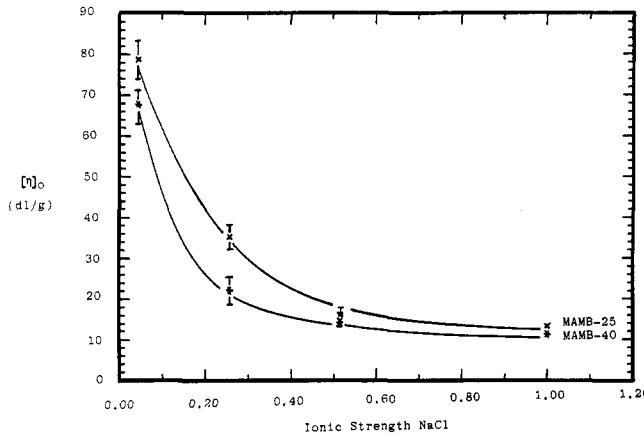


**Figure 3.** Effect of sodium chloride concentration on the zero-shear intrinsic viscosities of AM–NaMAMB copolymers at 30 °C.

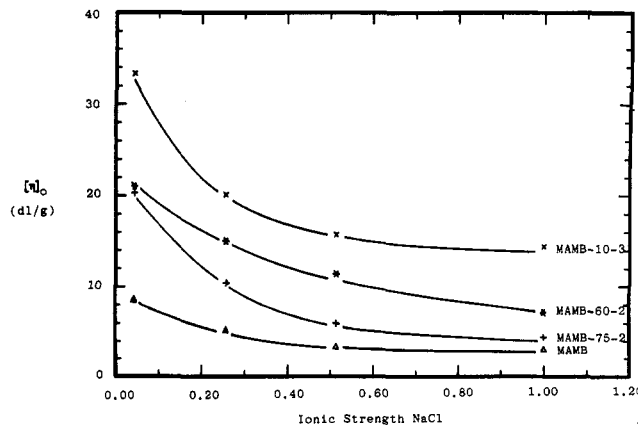


**Figure 4.** Effect of sodium chloride concentration on the zero-shear intrinsic viscosities of AM–NaMAMB copolymers and NaMAMB homopolymer at 30 °C.

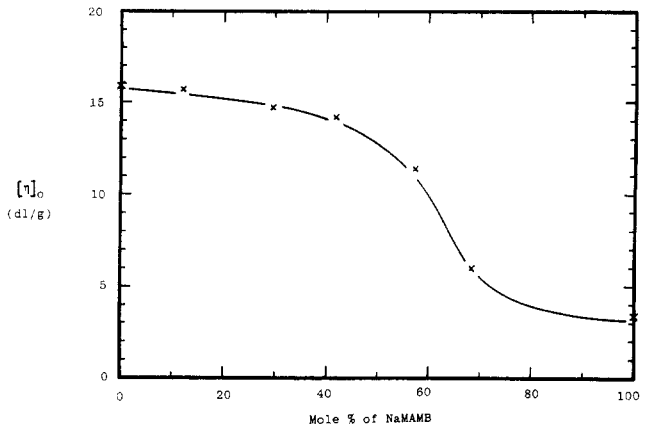


**Figure 5.** Compositional effect on zero-shear intrinsic viscosity in 0.514 M NaCl(aq) at 30 °C for AM–NaMAMB polymers.

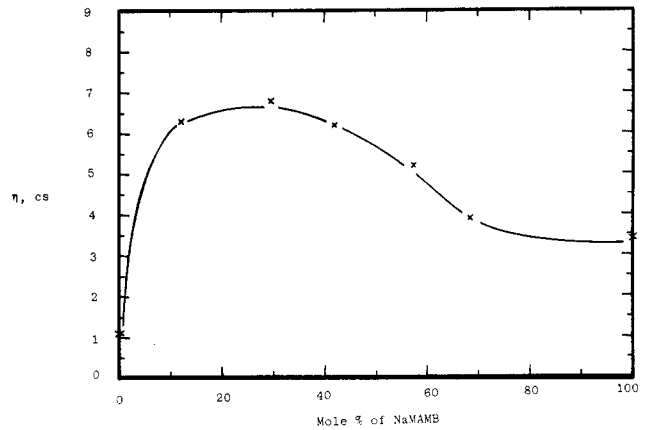


**Figure 6.** Compositional effect on viscosity in deionized water at 30 °C for AM–NaMAMB copolymers (polymer concentration = 0.015 g/dL, shear rate = 100 $s^{-1}$).

trations. At low ionic strengths, MAMB-25-3 and MAMB-40-3, which contain 30 and 42 mol % NaMAMB, respectively, exhibit the maximum viscosities (Figure 3). These high-solution viscosities may be attributed to maximum hydrodynamic size, which results from an optimum charge density as predicted by the Manning theory.[17]

The zero-shear intrinsic viscosities of the AM–NaMAMB polymers are found to decrease sharply with increasing ionic strength. Copolymers of AM with NaAMB previously studied in our laboratories were found to be significantly more tolerant to added electrolytes.[5] A possible explanation for the observed differences in salt sensitivities is that the presence of the $\alpha$-methyl group of NaMAMB introduces more hydrophobic character, resulting in decreased macromolecular size as a function of added electrolytes. Another contributing factor may be the differences in copolymer microstructure.

**Effects of Copolymer Composition.** The effects of copolymer composition on the zero-shear intrinsic viscosities of the AM–NaMAMB copolymers in 0.514 M NaCl and on the apparent viscosities of the polymers in deionized water are shown in Figures 5 and 6, respectively. The zero-shear intrinsic viscosities of the polymers in 0.514 M NaCl decrease with increasing NaMAMB content; however, the molecular weight also decreases with increasing NaMAMB content. It is therefore difficult to effectively partition viscosity loss due to structural and/or molecular weight changes.

It was not possible to obtain intrinsic viscosities for the AM–NaMAMB polymers in pure water by extrapolation to zero shear rate due to the overwhelming polyelectrolyte

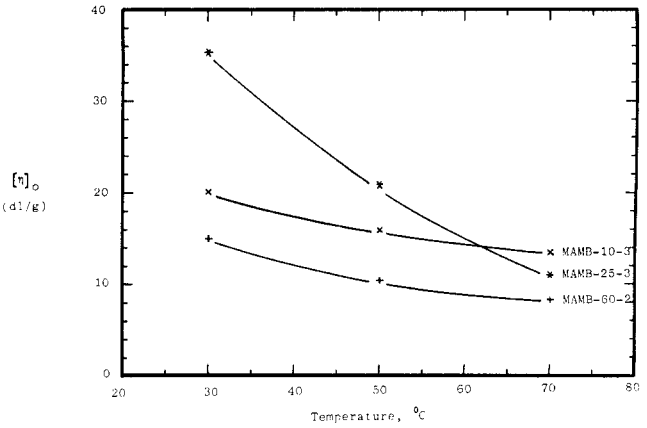


**Figure 7.** Zero-shear intrinsic viscosities of AM–NaMAMB copolymers in 0.257 NaCl(aq) as a function of temperature.

**Table II**
**Zero-Shear Intrinsic Viscosity Data for Copolymers of Acrylamide (AM) with Sodium 3-Methacrylamido-3-methylbutanoate (NaMAMB) in 0.514 M NaCl Solutions of Various pH Values at 30 °C**

| sample | mol % NaMAMB | pH | $[\eta]_0$, dL/g |
|---|---|---|---|
| MAMB-10-3 | 12.1 | 5 | 13.7 |
| | | 6 | 14.6 |
| | | 8 | 15.7 |
| MAMB-25-3 | 29.6 | 5 | 11.4 |
| | | 6 | 13.7 |
| | | 8 | 14.7 |
| MAMB-40-3 | 41.9 | 5 | 9.5 |
| | | 6 | 10.7 |
| | | 8 | 14.2 |
| MAMB-60-2 | 57.3 | 5 | 6.0 |
| | | 6 | 6.5 |
| | | 8 | 11.4 |
| MAMB-75-2 | 68.3 | 5 | 3.7 |
| | | 6 | 4.2 |
| | | 8 | 6.0 |

effects. However, a comparison of apparent viscosities at 100 $s^{-1}$ and a polymer concentration of 0.015 g/dL was made. A maximum in viscosity was found at a copolymer composition containing 30 mol % NaMAMB, even though that polymer had a lower molecular weight than the copolymer containing 12 mol % NaMAMB. The greater hydrodynamic size of MAMB-25-3 in pure water might be attributed to an optimum arrangement of functional groups, resulting in maximum extension of the macromolecular chain.

**Effects of Temperature.** The effects of temperature on the zero-shear intrinsic viscosities of representative AM–NaMAMB copolymers in 0.257 M NaCl are shown in Figure 7. The zero-shear intrinsic viscosities of the polymers decrease with increasing temperature, indicating a decrease in the hydrodynamic volume of the polymer molecules. This in turn indicates conformational and solvent associational changes occurring as a function of temperature.

**Effects of pH.** Since the copolymers of AM with NaMAMB contain a carboxylic acid moiety, the effects of pH on the zero-shear intrinsic viscosities should be significant. As the potentiometric results show, however, the carboxylate moiety is an unusually weak base (relative to NaAMB). Thus the effects of pH on the viscosities of the AM–NaMAMB copolymers are not as strong as might be expected. Table II illustrates the dependence of the intrinsic viscosities on pH for the copolymers of AM with NaMAMB. The zero-shear intrinsic viscosities increase as the pH increases, corresponding to an increasing degree of ionization of the carboxylic groups. This leads to more

Table III
MAMB Series: Correlation between $pK_a$ and Copolymer Sequence Distribution

| sample | $H_2O$ | | 0.36 M KCl | | | | |
|---|---|---|---|---|---|---|---|
| | $pK_a$ | $\Delta pK_a$ | $pK_a$ | $\Delta pK_a$ | $P_{ABA}$ | $P_{ABB}$ | $P_{BBB}$ |
| MAMB-10 | 4.52 ± 0.03 | 0.28 | 4.21 ± 0.04 | 0.07 | 0.901 | 0.096 | 0.002 |
| MAMB-25 | 4.97 ± 0.05 | 0.36 | 4.34 ± 0.04 | 0.06 | 0.743 | 0.237 | 0.019 |
| MAMB-40 | 5.59 ± 0.05 | 0.26 | 4.79 ± 0.03 | 0.11 | 0.574 | 0.367 | 0.058 |
| MAMB-60 | 5.93 ± 0.04 | 0.32 | 4.98 ± 0.04 | 0.11 | 0.338 | 0.486 | 0.175 |
| MAMB-75 | 5.81 ± 0.05 | 0.53 | 4.84 ± 0.04 | 0.16 | 0.167 | 0.483 | 0.348 |
| MAMB-hom | 6.24 ± 0.05 | 0.67 | 5.07 ± 0.05 | 0.23 | | | |

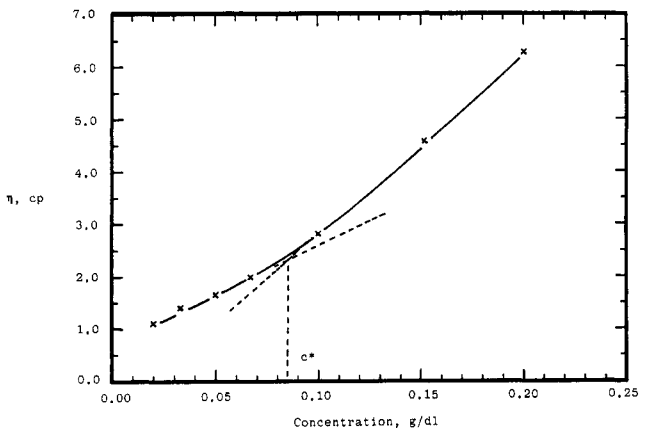


Figure 8. Effect of polymer concentration on viscosity in 0.514 M NaCl(aq) at 30 °C for MAMB-25-3 (shear rate = 1.7 $s^{-1}$).

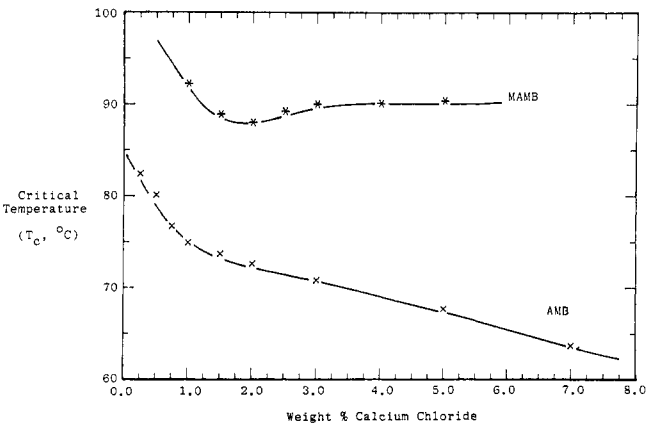


Figure 9. Comparison of the phase behavior of the NaMAMB (*) and NaAMB (×) homopolymers (polymer concentration = 1.5 g/L).

extended chain structures in solution due to electrostatic repulsions. (The pH studies were conducted in 0.514 M NaCl to provide appropriate counterion shielding of charged carboxylate units.)

**Effect of Polymer Concentration on Viscosity.** The effect of polymer concentration on viscosity for a typical copolymer of AM with NaMAMB (MAMB-25-3) is shown in Figure 8. The viscosities were obtained with a Contraves LS-30 rheometer at a shear rate of 1.7 $s^{-1}$ in 0.514 M NaCl. The critical overlap concentration $c^*$ was found to occur at a polymer concentration of 0.084 g/dL and is considered as that concentration at which effects due to chain entanglements first become apparent. The zero-shear intrinsic viscosity of MAMB-25-3 was determined to be 14.7 dL/g; thus, the product of the intrinsic viscosity and $c^*$ was found to be 1.2. At a polymer concentration above $c^*$, the solution is much more pseudoplastic in nature since chain entanglements are greatly affected by shear forces.

**Turbidimetry.** The AM–NaMAMB copolymers were found to behave similarly to the copolymers of acrylamide and sodium 3-acrylamido-3-methylbutanoate (NaAMB) in aqueous calcium chloride solutions.[5] No phase separation was observed for copolymers of AM and NaMAMB. Even the polymer containing 67 mol % NaMAMB units showed no phase separation behavior. The homopolymer of NaMAMB did show phase separation above 0.5% $CaCl_2$ concentration but only at temperatures above 85 °C. The phase behavior of the NaAMB and NaMAMB homopolymers is shown graphically in Figure 9.

Previous results[5,6,11,12] have shown that copolymers of acrylamide with comonomers with analogous structures to NaMAMB are very stable in aqueous solutions containing divalent ions. This unusual stability has been attributed to the geometry of the ions about the polymer chain, the microstructure of the copolymers, the hydrogen bonding with neighboring acrylamide units, the decreased ion binding capability of the charged group, and the stabilizing effects of the secondary amide of the NaAMPS and NaAMB comonomers.

Table IV
MAMB Series: Electrostatic Repulsions Calculated from the Modified Henderson–Hasselbalch Equation[a]

| sample | $pK_a$ | | $n$ | | $pK'$ | |
|---|---|---|---|---|---|---|
| | $H_2O$ | KCl | $H_2O$ | KCl | $H_2O$ | KCl |
| MAMB-10 | 4.52 | 4.21 | 1.4 | 1.0 | 4.53 | 4.21 |
| MAMB-25 | 4.97 | 4.34 | 1.6 | 1.0 | 4.97 | 4.33 |
| MAMB-40 | 5.59 | 4.79 | 1.6 | 1.0 | 5.57 | 4.78 |
| MAMB-60 | 5.93 | 4.98 | 1.5 | 1.1 | 5.93 | 4.98 |
| MAMB-75 | 5.81 | 4.84 | 1.9 | 1.1 | 5.81 | 4.84 |
| MAMB-hom | 6.24 | 5.07 | 2.1 | 1.2 | 6.24 | 5.07 |

[a] All correlation coefficients are 0.99.

The phase separation curve for the NaMAMB homopolymer is found to be 30–50 °C higher than for acrylamide–sodium acrylate copolymers. This increased stability can be explained by the structure of the NaMAMB repeat unit. The longer side chain of the NaMAMB unit increases the mobility of the anionic site. Moving the anionic site away from the backbone will effectively increase the distance between charges, thereby reducing the charge density on the chain and stabilizing the charge. The charge density is also decreased due to the alternating tendency of these copolymers.[18] This alternation increases the frequency of ABA triads in the copolymers and allows a greater degree of hydrogen bonding with adjacent AM units on the chain.

**Potentiometry.** The apparent $pK_a$ values for the AM–NaMAMB copolymers and the NaMAMB homopolymer are shown in Tables III and IV. The $pK'$ and $n$ values calculated from the modified Henderson–Hasselbalch equation (eq 1) are given in Table IV.

The titrations conducted in 0.36 M KCl give lower $pK_a$ values than those in pure water. This can be explained by the increased hydration of the charged groups in the presence of the added electrolytes and the increased local interaction due to the random coil formation of the chains caused by charge shielding. Greater conformational changes are observed in pure water due to the absence of charge shielding. The $pK_a$ vs. $\alpha$ curves in 0.36 M KCl and

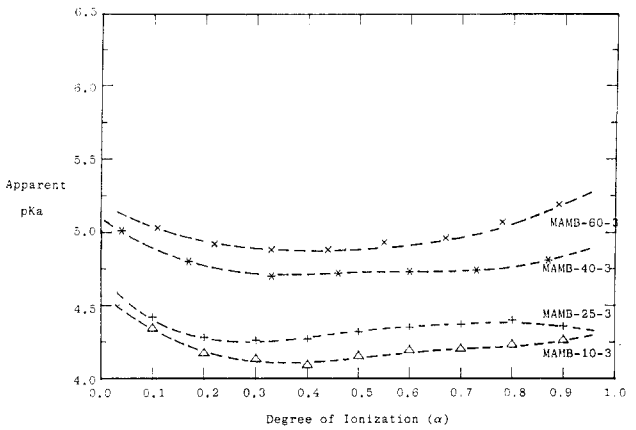


**Figure 10.** $pK_a$ vs. $\alpha$ plots for AM–NaMAMB copolymers in 0.36 M KCl (MAMB-10-3 (△); MAMB-25-3 (+); MAMB-40-3 (*); MAMB-60-3 (×)).

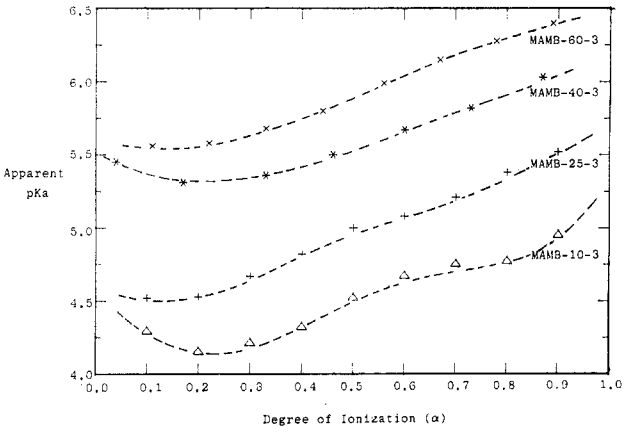


**Figure 11.** $pK_a$ vs. $\alpha$ plots for AM–NaMAMB copolymers in pure water (MAMB-10-3 (△); MAMB-25-3 (+); MAMB-40-3 (*); MAMB-60-3 (×)).

in pure water are shown in Figures 10 and 11.

Several trends can be observed in Table III. First, the $pK_a$ values tend to increase with increasing NaMAMB units in the copolymer. The increased charge density, which destabilizes the carboxylate groups, results in higher $pK_a$ values. Second, the $\Delta pK_a$ values also increase with increasing NaMAMB content, suggesting that the increased charge interactions cause increased conformational changes in the copolymers.

The copolymer sequence distributions and $pK_a$ values in Table III show certain trends as well. For the NaMAMB series, NaMAMB-centered triads can be categorized as ABA, BBA + ABB, or BBB, where A is an acrylamide unit on the polymer chain and B is a NaMAMB unit on the polymer chain. In Table III, $P_{ABA}$ is the probability that a NaMAMB-centered triad will have a NaMAMB unit flanked by an acrylamide unit on each side, while $P_{BBB}$ is the probability that a NaMAMB unit will be flanked by two NaMAMB units. $P_{ABB}$ is the probability that a NaMAMB unit will be flanked by one acrylamide and one NaMAMB unit. These probabilities are calculated based on reactivity ratios and copolymer composition data.[7] The NaMAMB copolymers have a strong alternating tendency as reflected in the unusually high frequency of ABA triads in the copolymers. The $pK_a$ values decrease with increasing ABA triads, apparently due to the increased availability of the neighboring acrylamide units for hydrogen bonding. This hydrogen bonding stabilizes the conjugate base form of the NaMAMB pendent units, giving them lower $pK_a$ values. The reverse trend is observed for BBB triads, where $pK_a$ values increase with

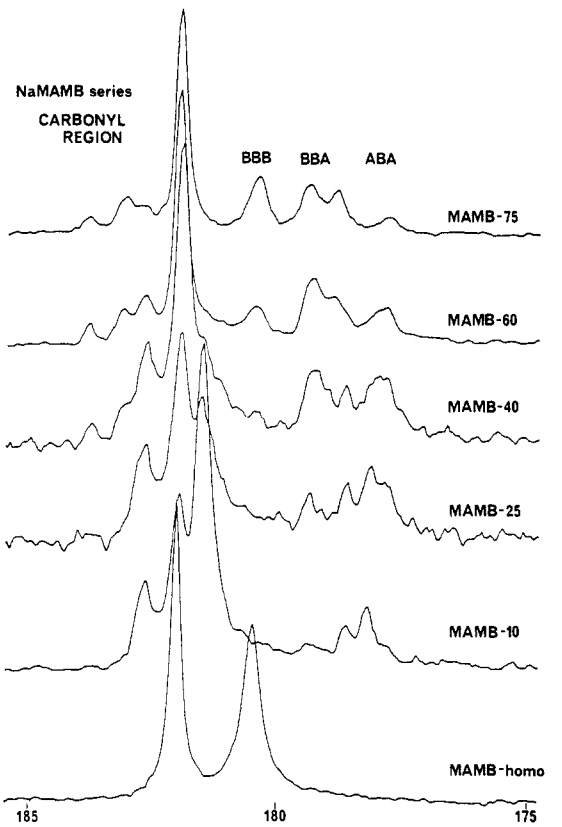


**Figure 12.** The 175–185 ppm region of the $^{13}C$ NMR spectra of the AM–NaMAMB copolymers and the NaMAMB homopolymer.

increasing BBB triad content due to the increased charge–charge repulsion. These data have been verified from NMR data that will be presented in the next section.

The electrostatic repulsions between the charged groups in the copolymers were studied with the modified Henderson–Hasselbalch equation. The $n$ value is a measure of the charge–charge interactions, where $n = 1$ is the standard taken for a monoacid. Values of $n > 1$ are caused by charge–charge repulsion along a polymer chain. Table IV gives the $n$ values and $pK'$ values for the NaMAMB series, as well as the $pK_a$ values calculated from the standard Henderson–Hasselbalch equation. Agreement between the two values is good.

The $n$ values are higher in pure water than the $n$ values in KCl solutions, as expected since the charge–charge interactions are masked by the added electrolytes in the KCl solutions. In pure water, the charge–charge repulsion is much greater, causing higher viscosities and more rodlike character of the polymer in solution as reflected in high $n$ values. In 0.36 M KCl (Table IV), values of $n = 1$ are observed, suggesting that each charged group is acting like a monoacid. In $H_2O$, however, the $n$ values increase with increasing NaMAMB content due to the increasing charge density of the copolymers.

**$^{13}C$ NMR Spectroscopy.** The NaMAMB copolymers give $^{13}C$ NMR spectra that show splitting in the carbonyl region, apparently due to the varying microstructures of the NaMAMB repeat units. The homopolymer carbonyls do not split, as shown in Figure 12. Thus, the observed splitting patterns are a result of local interactions and are consistent with those expected for triad sequences. The frequency of these change with changes in copolymer composition and copolymer sequence distributions (CSD).

In order to verify that the splitting patterns were caused by the inherent magnetic properties of the nuclei involved, attempts were made to obtain altered patterns by adjusting the pH and the ionic strength and by increasing the tem-

**Table V**
**Comparison of Calculated and Measured Copolymer Sequence Distributions**

| | $P_{ABA}$ | | | $P_{ABB}$ | | | $P_{BBB}$ | | |
|---|---|---|---|---|---|---|---|---|---|
| sample | calcd (ref 7) | NMR integ | anal. wt | calcd | NMR integ | anal. wt | calcd | NMR integ | anal. wt |
| MAMB-10 | 0.901 | 0.948 | | 0.096 | 0.052 | | 0.002 | 0.000 | |
| MAMB-25 | 0.743 | 0.935 | 0.864 | 0.237 | 0.065 | 0.134 | 0.019 | 0.000 | 0.002 |
| MAMB-40 | 0.574 | 0.597 | 0.580 | 0.367 | 0.350 | 0.359 | 0.058 | 0.053 | 0.062 |
| MAMB-60 | 0.338 | 0.259 | 0.275 | 0.486 | 0.544 | 0.523 | 0.175 | 0.197 | 0.202 |
| MAMB-75 | 0.167 | 0.125 | 0.129 | 0.483 | 0.522 | 0.527 | 0.348 | 0.353 | 0.344 |

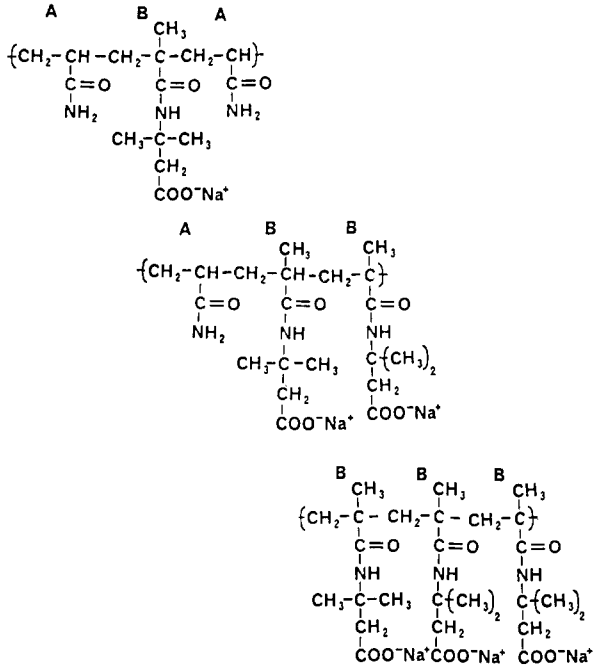

**Figure 13.** Representation of the three possible sequences for NaMAMB-centered triads.

perature of the sample solutions. However, pH changes in the solutions from 9 to 3.5 gave no effect on the splitting patterns. Also, the addition of NaCl up to concentrations of 3% had no effect. The spectra obtained at temperatures up to 90 °C still showed these splitting patterns. Thus, the observed splitting in the NaMAMB carbonyls is believed to be the result of differences in the local magnetic environments of the NaMAMB units. These microstructural differences are caused by interactions between acrylamide and NaMAMB units and not between two NaMAMB units, as evidenced by the lack of splitting in the homopolymer.

The splitting patterns are shown for the homopolymer and 5 copolymers of the NaMAMB series in Figure 12, where the region between 175 and 185 ppm has been expanded. The relative peaks areas were calculated in two ways: (1) standard NMR integration, and (2) analytical weight determination by cutting and weighing the respective peaks. These were compared to the statistical calculation of CSD for the copolymers in Table V. Figure 13 illustrates the three possible triad sequences.

The comparisons in Table V reveal that the splitting patterns observed in the copolymer spectra are directly related to CSD. Comparison of the calculated triad sequences and the measured splitting shows excellent agreement among the three methods. The data for MAMB-40, -60, and -75 show the best agreement due to the higher intensities of the NaMAMB carbonyl peaks, while the MAMB-10 and -25 spectra show less agreement due to the problems of low signal-to-noise ratio and lower intensities.

The peak assignments for the triads were made in the following way. The BBB peak (180.9 ppm) is expected to be at an equivalent chemical shift to the NaMAMB $COO^-$ peak in the homopolymer, which is 100% BBB triads. This can be seen in Figure 11. The remaining peaks at 178–179 ppm will be the ABA and ABB triad peaks. On the basis of potentiometric data discussed in the previous section, the ABA triads are expected to be the most stable acids or conjugate base forms due to their hydrogen bonding capability. Thus, it was assumed that the peak farthest upfield is the ABA peak. The results shown in Table V are based on these assumptions.

Some further splitting is seen in the ABA peak in MAMB-10 and -25 and in the ABB peak in MAMB-40, -60, and -75, which can be explained by differences in orientation and configuration in the various triads.

The NMR data, as in previous quantitative analyses, have an error margin of 5% due to broadening that is characteristic of NMR spectra of polymers.

## Conclusions

The AM–NaMAMB polymers have been shown to have moderate solution viscosities and good resistance to divalent ion binding. Furthermore, all of the NaMAMB polymers exhibited viscosity decreases with increasing temperature and decreasing pH. The NaMAMB polymers were found to be more sensitive to increasing ionic strength than copolymers of AM with NaAMB[6] due to increased hydrophobicity and microstructural differences. No significant aging effects were observed in salt solutions; however, in pure water, viscosity decreases up to 45% were observed as a function of time due to conformational changes.

The statistical method of Harwood and Ritchey for microstructural analysis has been experimentally verified by $^{13}C$ NMR. The microstructural analyses show an unusually high frequency of ABA triads due to the alternating tendency of the monomers. The $pK_a$ values of the NaMAMB polymers were found to be lower than comparable AM–NaAMB polymers due to the enhanced stability resulting from hydrogen bonding with nearest-neighbor AM units. The alternation in the copolymers, as well as the longer side chain of the NaMAMB unit, serves to decrease the effective charge density of the polymer, thereby stabilizing the anionic groups. The viscometric, turbidimetric, and potentiometric data suggest the importance of local interactions specified by copolymer microstructure. These include hydrogen bonding, hydrophobic, and steric interactions along the macromolecular chain.

**Acknowledgment.** Support for this research from the US Department of Energy under Contract No. DE-AS19-80BC10321 is gratefully acknowledged.

**Registry No.** (AM)·(NaMAMB) (copolymer), 101672-02-0; NaMAMB (homopolymer), 101672-03-1; NaCl, 7647-14-5.

## References and Notes

(1) Finch, C. A., Ed. *Chemistry and Technology of Water-Soluble Polymers*; Plenum: New York, 1983.
(2) Truong, D. N.; Galin, J. C.; Francois, J.; Pham, Q. T. *Polym. Commun.* **1984**, *25*, 208.
(3) Schwartz, T.; Francois, J. *Makromol. Chem.* **1981**, *182*, 2775.
(4) McCormick, C. L.; Blackmon, K. P., to be published in *J. Polym. Sci., Polym. Chem. Ed.*

(5) McCormick, C. L.; Blackmon, K. P.; Elliott, D. L., to be published in *J. Polym. Sci., Polym. Chem. Ed.*
(6) McCormick, C. L.; Elliott, D. L. *Macromolecules* **1986**, *19*, 542.
(7) Harwood, H. J.; Ritchey, S. *Polym. Lett.* **1964**, *2*, 601.
(8) Igarashi, S. *J. Polym. Sci., Polym. Lett. Ed.* **1963**, *1*, 359.
(9) Carreau, P. J.; Dekee, D.; Daroux, M. *Can. J. Chem. Eng.* **1979**, *57*, 135.
(10) Billmeyer, F. W. *Textbook of Polymer Science*, 2nd ed.; Wiley Interscience: New York, 1971; p 86.
(11) Arai, F. Master's Thesis, University of Southern Mississippi, Hattiesburg, MS, 1984.
(12) Neidlinger, H. H.; Arai, F. *DOE Contract No. DE-AS19-80BC10321, Fifth Annual Report*, 1982.
(13) Tan, J. S.; Gasper, S. P. *Macromolecules* **1973**, *6*, 741.
(14) Katchalsky, A.; Spitnik, P. *J. Polym. Sci.* **1947**, *2*, 432.
(15) Kulicke, W. M.; Kniewske, R. *Makromol. Chem.* **1980**, *181*, 823.
(16) Kulicke, W. M.; Kniewske, R. *Makromol. Chem.* **1981**, *182*, 2277.
(17) Manning, G. S. *Acc. Chem. Res.* **1979**, *12*, 443.
(18) McCormick, C. L.; Blackmon, K. P. *Macromolecules*, preceding paper in this issue.

# Polymer Swelling. 5. Correlation of Relative Swelling of Poly(styrene-*co*-divinylbenzene) with the Hildebrand Solubility Parameter of the Swelling Liquid

**L. A. Errede**

*3M Science Research Laboratories of Central Research, 3M Center, Building 201-2N-22, St. Paul, Minnesota 55144.* *Received October 17, 1985*

ABSTRACT: The swellability, $S$, of styrene-*co*-divinylbenzene polymers in 20 aromatic and 24 aliphatic liquids was studied as a function of cross-link density, $\lambda^{-1}$, from $\lambda^{-1} = 0.01$ to $\lambda^{-1} = 0.12$. In every study the relationship was given by $S = C(\lambda^{1/3} - \lambda_0^{1/3})$, where $\lambda$ is the average number of carbon atoms in the "backbone" of the polystyrene segments between cross-link junctions, $C$ is the relative swelling power of the liquid, and $\lambda_0^{-1}$ is the critical cross-link density, above which $S = 0$. The observed $C$ was correlated with the corresponding known Hildebrand solubility parameter, $\delta$, for five liquid classifications. The solubility parameter of the polymer, $\delta_{Sty}$, determined thereby was 9.5 for substituted benzenes, 9.2 for chlorocarbons, 9.1 for ketones, 8.4 for esters, and 7.3 for ethers. this set of observed $\delta_{Sty}$ spans the range reported by earlier investigators, i.e., $\delta_{Sty} = 8.6$–$9.7$. The plots of $C$ as functions of the corresponding $(\delta_{Sty} - \delta_{liq})^2$ for the homologous series of liquids $Z(CH_2)_nH$, where $n < 5$, are almost parallel lines given approximately by $C = A - 0.60(\delta_{Sty} - \delta_{liq})^2$, where $A$ is 2.19 for Z = Ph, 1.48 for Z = $RCO_2$, 1.42 for Z = RCO, and 0.64 for Z = RO. Apparently, the major factor that determines swelling power is the relative affinity of Z for the polymer. The cumulative contribution to swelling power owing to the $(CH_2)_nH$ group is only a mitigating factor superimposed on the former.

## Introduction

We reported[1] that the magnitude of swelling of a polymer, $S$ (in milliliters of liquid absorbed per gram of polymer in equilibrium with excess liquid), can be measured conveniently and reproducibly after the polymer is comminuted and then fabricated into a thin (<0.3 mm), but tough (tensile strength >250 psi), microporous (>0.5 porosity) composite membrane consisting of the particulate polymer (>80% by weight) enmeshed in poly(tetrafluoroethylene) microfibers (<20%). We correlated $S$ with the corresponding cross-link density, $\lambda^{-1}$, of styrene-*co*-divinylbenzene polymers, which ranged from $\lambda^{-1} = 0.01$ to $\lambda^{-1} = 0.12$, and we showed[2,3] that $S$ is related to $\lambda^{-1}$ by

$$S = C(\lambda^{1/3} - \lambda_0^{1/3}) \quad (1)$$

where $\lambda$ is the average number of carbon atoms in the backbone of the polystyrene segments between cross-link junctions, $\lambda_0^{-1}$ is the critical cross-link density of the polymer, above which $S = 0$, and $C$ is the relative swelling power of the liquid.

It is well-known that swelling power is related to solvent power,[4] which can be expressed in terms of the Hildebrand solubility parameter,[5] $\delta$, and that the solubility of a given solute with solubility parameters $\delta_{sol}$ in a given liquid with solubility parameter $\delta_{liq}$ is maximal when $(\delta_{sol} - \delta_{liq})^2$ is zero. Gee[6] has shown that a similar relationship appears to obtain for swelling of cross-linked polymers; i.e., swelling is maximal when $(\delta_p - \delta_{liq})^2$ is zero, where $\delta_p$ is the solubility parameter of the polymer. It was of interest, therefore, to attempt measurement of $\delta_{Sty}$ for poly(Sty-*co*-DVB) on the basis of the swelling power, $C$, observed by us as a function of the corresponding $\delta_{liq}$ reported by others[7-10] and then to compare the observed $\delta_{Sty} = \delta_{liq}$ at $C_{max}$ with the corresponding $\delta_{Sty}$ determined experimentally by others[7,8,11-13] on the basis of maximal solubility. The latter varied from $\delta_{Sty} = 8.6$ to 9.7 in $cal^{1/2}/cm^{3/2}$.

The purpose of this publication is to report the results of our correlation that was aimed at a possible explanation for the wide range of $\delta_{Sty}$ observed experimentally by earlier investigators.

## Experimental Section

The procedure for making thin microporous composite films from poly(Sty-*co*-DVB) particular and PTFE emulsion is described[1] in detail in part 1. The procedure for measuring $S$, in milliliters of absorbed liquid per gram of polymer, is described[2] in detail in part 2. The set of six composite films that were used previously to study $S$ as a function of $\lambda^{1/3}$ in 19 organic liquids (Table 1 of ref 2) were again used to establish the characteristic linear relationship (Figures 3 and 4 of ref 2) for the 20 aromatic and 24 aliphatic liquids listed in Tables I and II. The liquids tested were obtained from commercial sources, usually Aldrich Chemical Co., and they were used without further purification.

## Results and Discussion

The 44 compounds listed in Tables I and II were selected for this correlation of poly(Sty-*co*-DVB) swelling power, $C$, with the corresponding Hildebrand solubility parameter, $\delta$, on the basis of the following criteria: (1) the melting point of the compound was <20 °C and the boiling point was >40 °C; (2) the corresponding Hildebrand solubility parameter of the liquid was published in the scientific

0024-9297/86/2219-1522$01.50/0 